# SCANNING FLUORESCENCE CORRELATION SPECTROSCOPY

## II. Application to Virus Glycoprotein Aggregation

N. O. PETERSEN,* D. C. JOHNSON,[‡] AND M. J. SCHLESINGER[§]

*Department of Chemistry, The University of Western Ontario, London, Ontario, Canada N6A 5B7;
[‡]Cancer Research Group, Department of Pathology, McMaster University, Hamilton, Ontario L8N
3Z5; and [§]Department of Microbiology and Immunology, Washington University School of Medicine,
St. Louis, MO 63110

ABSTRACT  Scanning fluorescence correlation spectroscopy is a new approach to measuring changes in the state of aggregation of cell membrane proteins. Measurements of the mean number of aggregates of virus glycoproteins from Sindbis virus and vesicular stomatitis virus agree with the findings of a recent fluorescence photobleaching recovery study on the same systems (Johnson, D. C., M. J. Schlesinger, and E. L. Elson, 1981, *Cell*, 23:423–431). Sindbis Virus glycoproteins are immobilized and cannot be induced to aggregate further by antibody cross linking. In this study, we find that Sindbis virus glycoprotein is more highly aggregated than vesicular stomatitis virus glycoprotein, which can be patched further with antibody. These measurements demonstrate the potential of scanning fluorescence correlation spectroscopy in studies of aggregation problems in membranes of cultured cells.

## INTRODUCTION

Membrane-enveloped animal virus particles emerge from the infected host cell by a budding process (1) that varies in detail between virus classes. Common features include assembly of virally coded membrane glycoproteins, nucleocapsid proteins, and nucleic acids into membrane patches, which evaginate and incorporate host cell membrane lipids in the process. Host cell membrane proteins are for the most part excluded from the virus particles.

Fluorescence photobleaching recovery (FPR) measurements of diffusion and mobile fractions of virus glycoproteins have been employed to study the mechanism of virus budding for two viruses: vesicular stomatitis virus (VSV) and Sindbis virus (SbV) (2, 3). These studies suggested different budding mechanisms for the two virus types. The VSV data are consistent with a dispersed and mobile distribution of glycoprotein that incorporates into buds by aggregation. The SbV data are consistent with a more aggregated and immobile distribution of glycoprotein, particularly late in the infection cycle. The latter findings are in accord with electron microscopy studies that suggest that SbV glycoprotein is inserted in the host cell membrane in pre-assembled aggregates, already associated with the nucleocapsid (4).

Fluorescence correlation spectroscopy (FCS) measurements are sensitive to the number of fluorescent particles in the observation volume (5–8) and can, in principle, be used to study aggregation problems. In an accompanying article (9) we introduced scanning fluorescence correlation spectroscopy (S-FCS) as an adaptation of FCS to measure aggregation in systems where diffusion is slow. We showed that S-FCS measurements can provide estimates of the mean number of aggregates per unit area and, in favourable cases, the mean number of monomers per aggregate.

Here we report on the application of S-FCS experiments in a study of the distribution of virus glycoproteins on surfaces of infected cells. The aggregation data are consistent with the FPR measurements reported previously for the same virus and cell systems (3). The experiments provide an example of the potential use of S-FCS measurements in studies of cell membrane aggregation processes.

## METHODS

Tetramethylrhodamine derivatized rabbit antibodies specific for glycoproteins from Sindbis virus ($\alpha$SbV) and vesicular stomatitis virus ($\alpha$VSV) were prepared previously (3, 4). Chick embryo fibroblasts (CEF) were infected with wild type (wt) and mutant (ts-20) SbV and BHK-21 (BHK) cells were infected with VSV as described (3).

Infected cells, cultured on glass coverslips, were washed with cold buffer (phosphate buffered saline with 1 mM $CaCl_2$ and 1 mM $MgCl_2$ at pH 7.4), cooled to 4°C on ice to stop the progress of the infection and then labeled with 100 $\mu$g pre-adsorbed fluorescent antibody in 100 $\mu$l for 30 min. Pre-adsorbed antibody was obtained by incubation with noninfected cells several times to minimize nonspecific binding. In some samples, antibody that was not pre-adsorbed was used on infected cells as an indication of the nonspecific binding (ns in Fig. 3). After incubation, the cells were washed 4–5 times with cold buffer, warmed to room temperature, and fixed with 1% paraformaldehyde in the buffer for 10 min. In some experiments with SbV the cells were incubated with $\alpha$-rabbit-IgG at room temperature before fixing to induce cross linking of mobile glycoproteins bearing $\alpha$SbV. In an experiment with VSV, the glycoproteins were allowed to aggregate by incubation at room temperature through cross linking by the $\alpha$VSV. All samples were mounted, inverted, and in glycerol.

Scanning fluorescence correlation spectroscopy experiments were performed as described in the accompanying article (9). The scan was achieved in 1,024 steps covering a total range of 32 $\mu$m using a count time per channel of 40 ms. The sample was illuminated with the 528.7 nm laser line from an Argon-ion laser employing a beam radius at the sample of $w = 0.9$ $\mu$m. The laser power at the sample was less than a microwatt and no photobleaching was observed during the measurements, in part because of the short exposure on the moving sample.

The fluorescence intensity data records were analyzed by calculation of the normalized autocorrelation function $g(k\Delta x)$ (Eq. 8 in reference 9), where $k$ is the data channel separation and $\Delta x$ is the step resolution (displacement per channel; here $\Delta x = 32$ nm). The zero-time value, $g(0)$, was estimated from a three-parameter fit to the relation (9, 10)

$$g(k \cdot \Delta x) = g(0)e^{-(k\Delta x/w)^2} + g_o, \tag{1}$$

where $w$ is the characteristic beam radius and $g_o$ is an empirical offset value that accounts for low frequency statistical noise at large $k$-values. The first 50 correlation data points were used in the fit. Photographs were obtained on Kodak Tri-X film developed at 800 ASA.

## RESULTS

Fig. 1 illustrates the fluorescence distribution pattern on CEF cells infected with wild type (wt) SbV at early ($A$) and late ($B$) stages of the infection as well as with ts-20 before ($C$) and after ($D$) incubation with second antibody to induce further patching. The fluorescence staining

reveals a punctate pattern of SbV glycoproteins, indicating an aggregated distribution. It is difficult to assess unambiguously which distribution is more highly aggregated. Objective evaluation of these photographs are further hampered by the shallow depth of focus at the high magnification (100 oil immersion objective). Fig. 2 shows a pair of photographs of the same cells but focused either at the base of the cells ($A$) or at the top of the cells ($B$). The distributions appear different because of the diffuse fluorescence imaged from the out-of-focus membrane. This is a well-known problem that limits the quantitative use of fluorescence photography or video image microscopy.

Fluorescence intensity measurements in FPR and S-FCS experiments are less sensitive to the variation in membrane position relative to the focal plane (11). More importantly, simulation studies of S-FCS experiments (9) show that the $g(0)$ parameter is only slightly, but systematically, affected by cell contour. The mean aggregate density calculated from S-FCS measurements, therefore, provides an objective estimate of the aggregation distribution. Such estimates are particularly good for comparison of aggregation or changes in aggregation.

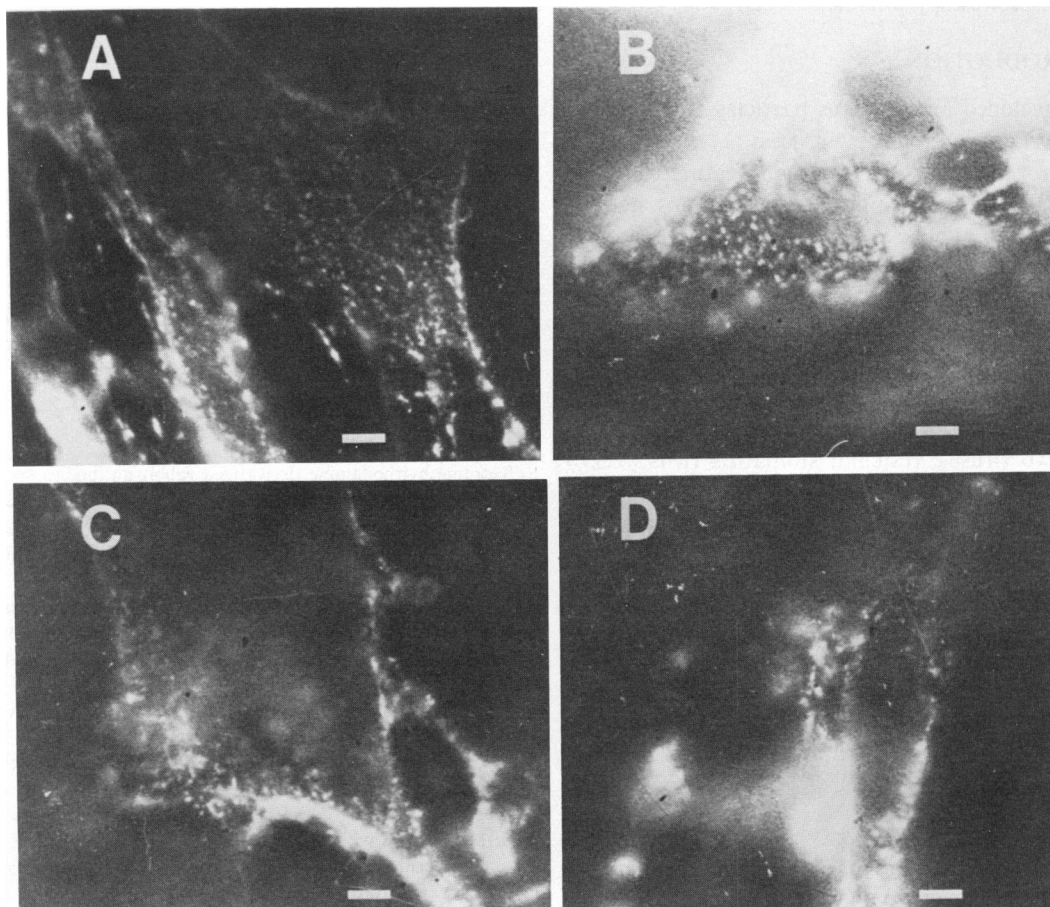The $g(0)$ parameter estimated from S-FCS experiments



FIGURE 1   Examples of the punctate fluorescence arising from binding of tetramethylrhodamine labelled antibody directed against SbV glycoproteins to cells infected with wt-SbV for four hours ($A$) and nine hours ($B$) and for cells infected with ts-20 — SbV before ($C$) and after ($D$) incubation with second antibody to induce cross-linking. The bar corresponds to ~10 $\mu$m.
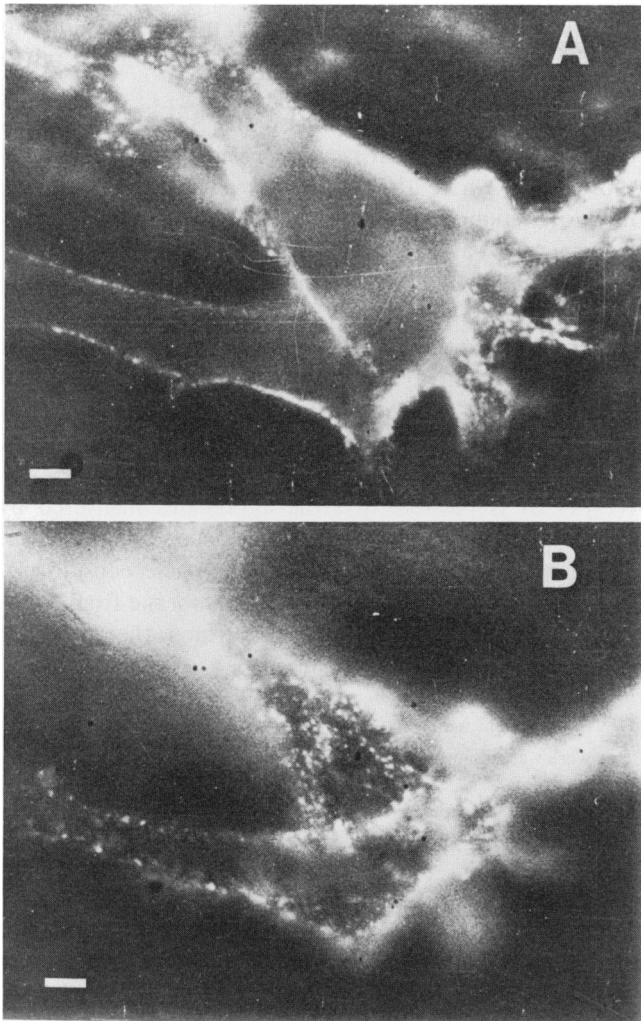
FIGURE 2  CEF infected with *wt*-SbV for 4 h and labeled with tetrame-thylrhodamine derivatized αSbV. Photographs *A* and *B* are of the same cells. In *A* the focal plane of the microscope was adjusted to coincide with the adherent surface (i.e., that closest to the glass coverslip) of the cell. In *B* the focal plane is at the top surface of the cell. Clearly the narrow depth of focus causes the appearance of evenly distributed fluorescence except for the membrane in focus where a punctate distribution is observed. The bar corresponds to ~10 μm.
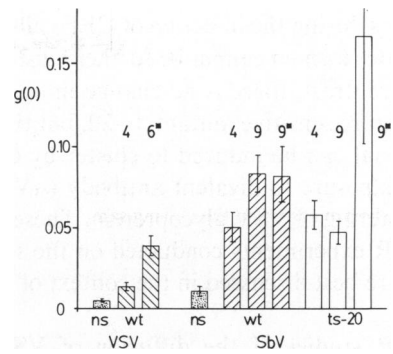


FIGURE 3  Graphical display of the average $g(0)$ value obtained from S-FCS experiments on BHK or CEF cells infected with VSV and SbV, respectively, ns, wt, and ts-20 refers to nonspecific, wild type and the *ts*-20 mutant of SbV. The number by each bar is the infection time in hours. The asterisk (*) indicates samples exposed to antibody that could induce further cross-linking as explained in the text.

is sensitive to the state of aggregation of the fluorescent molecules being observed. In the simplest case of unimodal distributions, $g(0)$ is inversely proportional to the number of aggregates: $g(0) = 1/\overline{N}_a$ (9, 10). Thus disperse receptor distributions would yield small $g(0)$ values while highly aggregated distributions yield large $g(0)$ values. In systems where mobile and immobile receptor aggregates coexist, $g(0)$ can be related to the fraction of mobile receptors $X_m$, as $g(0) = n/\overline{N}_m(1 - X_m)$, where $n$ is the number of monomers per aggregate and $\overline{N}_m$ the mean number of monomers. Thus we expect $g(0)$ to increase as the mobile fraction decreases.

Fig. 3 compares the $g(0)$ values obtained from S-FCS experiments on VSV-infected BHK cells and SbV-infected CEF cells. In both cases nonspecific (ns) labeling was obtained with nonadsorbed antibody on infected cells. The

preadsorption removes ~80% of the antibody. The aster-isks (*) mark experiments in which the virus glycoproteins were induced to aggregate by cross linking with a second antibody (for SbV) or by further incubation (for VSV).

Nonspecifically (ns) bound antibody is less aggregated than specifically bound antibody. The larger $g(0)$ value for the ns sample with SbV-infected cells compared to the ns sample with VSV-infected cells is a reflection of the ~20% specific binding in the nonadsorbed antibody preparation.

The $g(0)$ value for VSV at 4 h on BHK cells is smaller than that for SbV, indicating a more disperse distribution of VSV glycoproteins since (9, 10) $g(0) \simeq 1/\overline{N}_a$, where $\overline{N}_a$ is the mean number of aggregates in the beam area.

The $g(0)$ value increases during the infection between 4 and 9 h for the wt SbV-infected CEF cells suggesting an increase in the extent of aggregation or a smaller number of aggregates. This increase in $g(0)$ is observed in spite of an overall increase in density of virus glycoprotein on the cell surface during this time (3) (the fluorescence intensity increases by nearly 50%). There is, therefore, a real increase in the aggregate size that perhaps includes clus-ters of budding particles. The $g(0)$ value remains unchanged during the infection between 4 and 9 h for ts-20 SbV-infected CEF cells at a value comparable to that for the wild type virus at early times.

The $g(0)$ values increase when further aggregation is induced by antibody cross linking (marked by *) but only in those systems where FPR data (3) indicate that there are mobile glycoproteins. Specifically, the $g(0)$ value increases about three times for both VSV and ts-20 infected cells, but remains unchanged for wt infected cells after cross linking.

## DISCUSSION

The results presented here demonstrate that S-FCS experi-ments are sensitive to changes in virus glycoprotein aggre-gation in cell membranes. Specifically bound antibody is more clustered than the nonspecific controls for both αVSV and αSbV. There is a decrease in the mean number

of aggregates during the infection of CEF cells by SbV and the aggregates formed cannot be further clustered by cross linking. In contrast, there is no change in aggregation for the temperature sensitive mutant, ts-20, but the less aggregated material can be induced to cluster by cross linking. Similarly, exposure to divalent antibody ($\alpha$VSV) induces further clustering of VSV glycoprotein. These results fully support FPR experiments conducted on the same systems (2, 3) and are best discussed in the context of the diffusion data.

Two FPR studies of the diffusion of VSV and SbV glycoproteins have been reported (2, 3). The results are mutually consistent and the data relevant to the present work can be summarized as follows: the G-protein of VSV diffuses rapidly ($D \sim 5 \times 10^{-10}$ cm$^2$ s$^{-1}$) and most is mobile (mobile fraction, $X_m \sim 0.75$) under normal conditions (2). The mobile fraction is reduced in cells infected with virus mutants that have defective matrix (M) proteins, but the diffusion of the residual mobile glycoprotein remains rapid. The results for the wild type VSV were confirmed in the comparative study with SbV (3). The results are interpreted (2, 3) as support for a virus budding model in which G-proteins, after insertion into the host surface membrane, can diffuse and distribute randomly. Mobile G-protein can subsequently associate with M-protein and nucleocapsids forming aggregates that will, unless the M-protein is defective, rapidly form buds. The E$_1$ and E$_2$ glycoproteins of SbV also diffuse rapidly ($D \sim 6 \times 10^{-10}$ cm$^2$ s$^{-1}$), but typically less than half is mobile even early in the infection [3]. As the time of infection increases the mobile fraction decreases to <0.1, at which point it becomes impossible to measure the diffusion coefficient with any accuracy. Diffusion of E$_1$ and PE$_2$ glycoproteins (the transformation of the precursor PE$_2$ to E$_2$ is blocked in ts-20) in cells infected with ts-20 SbV is rapid and occurs with a large mobile fraction ($X_m \simeq 0.7$) at all times after infection at the nonpermissive temperature (39.5°C). These findings are consistent with a highly aggregated distribution of glycoproteins late in the infection cycle (3), and are in accord with the proposal (4) that SbV glycoproteins are inserted in the host cell membrane in preassembled aggregates. Electron microscopy data indicates that these are probably already associated with the nucleocapsid. The rapid diffusion at early times and for the ts-20 mutant implies that some of the glycoprotein may dissociate from the aggregates. The kinetics of virion release (3) suggest that the "leakage" of proteins from the buds to the membrane is irreversible, and therefore these glycoproteins do not participate in bud formation later in the infection.

In this context, the S-FCS measurements demonstrate that the decrease in the fraction of mobile SbV glycoproteins corresponds to an increase in the extent of aggregation of virus glycoproteins as expected from the relation (9), $g(0) = n/\bar{N}_m(1 - X_m)$. This represents the first direct link between immobilization and aggregation of membrane receptors: the fraction of immobile receptors is an indirect measure of the degree of aggregation in this system. This is reasonable and was in fact implicit in the previous interpretations (2, 3).

The S-FCS measurements also demonstrate that cross-linking receptors to increase aggregation is only possible in those cases where the FPR experiments show a large mobile fraction (VSV and ts-20 SbV). This is not surprising since the aggregation kinetics must depend on the collision frequency of the receptors and therefore on their ability to diffuse.

The aggregates of SbV glycoproteins are large since there are less than 10 aggregates per square micrometer on the cell surface. Although electron microscopic images can be difficult to quantitate, the density of virions on the cell surface appears to be greater than 10 per square micrometer (4). It is possible that the aggregates measured by S-FCS represents clusters of virus buds, which is what would be expected if the glycoprotein-nucleocapsid complexes are inserted into the plasma membrane from intracellular vesicles by fusion. After fusion the immobile complexes would remain clustered.

## REFERENCES

1. Lenard, J., and R. W. Compans. 1974. The membrane structure of lipid-containing viruses. Biochim. Biophys. Acta. 344:51–94.

2. Reidler, J. A., P. M. Keller, E. L. Elson, and J. Lenard. 1981. A fluorescence photobleaching study of vesicular stomatitis virus infected BHK cells. Modulation of G protein mobility by M protein. Biochemistry. 20:1345–1349.

3. Johnson, D. C., M. J. Schlesinger, and E. L. Elson. 1981. Fluorescence photobleaching recovery measurements reveal differences in envelopment of sindbis and vesicular stomatitis viruses. Cell. 23:423–431.

4. Johnson, D. C., and M. J. Schlesinger. 1980. Vesicular stomatitis virus and sindbis virus glycoprotein transport to the cell surface is inhibited by ionophores. Virology. 103:407–424.

5. Elson, E. L., and D. Magde. 1974. Fluorescence correlation spectroscopy. I. Conceptual basis and theory. Biopolymers. 13:1–27.

6. Magde, D., E. L. Elson, and W. W. Webb. 1974. Fluorescence correlation spectroscopy. II. An experimental realization. Biopolymers. 13:29–61.

7. Elson, E. L., and W. W. Webb. 1975. Concentration correlation spectroscopy: A new biophysical probe based on occupation number fluctuations. Annu. Rev. Biophys. Bioeng. 4:311–334.

8. Weissman, M. B. 1981. Fluctuation spectroscopy. Annu. Rev. Phys. Chem. 32:205–232.

9. Petersen, N. O. 1986. Scanning fluorescence correlation spectroscopy. I. Theory and simulation of aggregation measurements. Biophys. J. 49:809–815.

10. Petersen, N. O. 1984. Diffusion and aggregation in biological membranes. Can. J. Biochem. Cell. Biol. 62:1158–1166.

11. Petersen, N. O., and W. B. McConnaughey. 1981. Effects of multiple membranes on measurements of cell surface dynamics by fluorescence photobleaching. J. Supramol. Struct. Cell. Biochem. 17:213–221.